

Bioelectrochemistry and Bioenergetics, 20 (1988) 45–56
 A section of *J. Electroanal. Chem.*, and constituting Vol. 254 (1988)
 Elsevier Sequoia S.A., Lausanne – Printed in The Netherlands

Scanning curves and kinetics of the acetylcholine / acetylcholine receptor hysteresis [★]

Eberhard Neumann ^{★★}, Elvira Boldt, Barbara Rauer and Hendrik Wolf

Faculty of Chemistry, University of Bielefeld, P.O. Box 8640, D-4800 Bielefeld 1 (F.R.G.)

Hai Won Chang

Department of Neurology, College of Physicians and Surgeons, Columbia University, New York, NY 10032 (U.S.A.)

(Received 5 October 1987)

ABSTRACT

The high affinity binding of the neurotransmitter acetylcholine (AcCh) to the nicotinic acetylcholine receptor (nAChR) of the electric organ of *Torpedo californica* exhibits a pronounced hysteresis and scanning loops. Dialysis conditions lead to an equilibrium binding curve which is coincident with the upper hysteresis branch; $\bar{K} = 5 \times 10^{-9} M$, 4°C; and one AcCh molecule binds to the receptor (R) monomer of $M_r \approx 290000$. Kinetic analysis of the changes in free and bound AcCh during the open-system conditions of dialysis, which releases the metastability, shows that AcCh (A) binding proceeds along an *induced-fit* pathway according to $A + R_h \rightleftharpoons AR_h \rightleftharpoons AR_{vh}$, describing the ligand-induced transition from the high affinity state (R_h ; $K_h \approx 10^{-7} M$) to the very high affinity state (R_{vh} ; $K_{vh} \ll \bar{K}$). The rate constant of the step $AR_h \rightarrow AR_{vh}$ is $k_2 = 6 \times 10^{-3} s^{-1}$ and that of the reverse step is $k_{-2} = 3 \times 10^{-4} s^{-1}$. Direct binding of A to free R_{vh} can be neglected. Therefore, the state R_{vh} *does not pre-exist*; it is induced and only stable, as AR_{vh} , by bound AcCh. The metastability can be described in terms of long-lived $AR_{vh} \cdot R_1$ hybrid dimers. Physiologically, the steric hindrance in the metastable hybrid may be viewed as a saving device: the functionally important, receptor channel-active R_1 conformer is, at low AcCh concentrations ($[A] < 1 \mu M$), prevented from converting into the desensitized states R_h and AR_{vh} .

INTRODUCTION

The synaptic neurotransmitter acetylcholine (AcCh) binds to the nicotinic acetylcholine receptor of *Torpedo californica* electrocytes along a hysteresis loop [1].

[★] Presented at the 9th BES Symposium on Bioelectrochemistry and Bioenergetics, Szeged (Hungary), 1–5 September 1987.

^{★★} To whom correspondence should be addressed.

Since AcCh is a cation $[(\text{CH}_3)_3\text{N}^+-\text{CH}_2\text{CH}_2\text{OCOCH}_3]$ and the receptor protein at pH 7 is net anionic, the hysteresis may be caused by mainly *electrostatic* contributions, similar to the case of the proton-binding hysteresis of certain polynucleotide complexes [2,3]. Because hysteresis is a physical mechanism for memory imprint [4–6] it is very tempting to associate synaptic AcCh hysteresis with neural memory processes.

AcCh binding hysteresis is obtained when *T. californica* membrane fragments rich in the nicotinic acetylcholine receptor (nAcChR) are mixed with AcCh of increasing concentration (pulse mode addition of AcCh) up to $[A] \approx 1 \mu\text{M}$, yielding the lower branch, followed by a gradual dilution of AcCh resulting in the upper branch of the hysteresis loop (see Fig. 1). If, however, AcCh binding is studied under the open-system conditions afforded by equilibrium dialysis, a concentration–dilution cycle always traces the upper curve. Although the binding of the pulse mode addition is time-independent (≥ 17 h, 4°C), it is only the upper curve that reflects true equilibrium binding [1].

Because the rapid, pulse-like addition of AcCh to nAcChR leads to less binding, receptor binding sites R_1 of lower affinity are preserved. Indeed, it is known that in the range of acetylcholine concentration $[A] \leq 1 \mu\text{M}$ where hysteresis is observed, only the high affinity receptor conformers, and not the low affinity ones, of the conformational equilibria ($R_1 \rightleftharpoons R_h$) are the targets of AcCh binding. Obviously, the extent to which the conformational equilibria are shifted to the side of the high

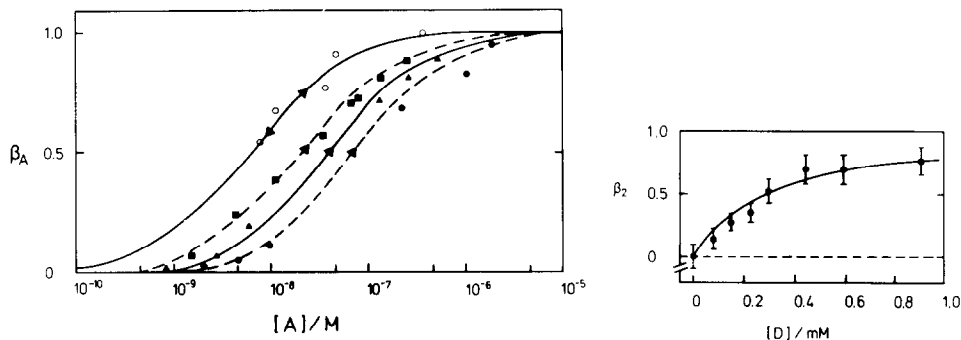


Fig. 1. The hysteresis of the high affinity acetylcholine binding to *T. californica* nAcChR in membrane fragments at 4°C . (○) Equilibrium dialysis data of $[^3\text{H}]\text{AcCh}$ binding, $[R_T] = 0.4 \mu\text{M}$; the curve was calculated using $\beta_A = [A]/([A] + \bar{K})$, with $\bar{K} = (5 \pm 1) \times 10^{-9} \text{M}$. (■, ▲, ●) Pulse mode addition (mixing) of $[^3\text{H}]\text{AcCh}$ at total receptor concentration $[R_T] = 0.1, 0.4$ and $1.0 \mu\text{M}$, respectively (α -Btx sites in the absence of detergent). The data have been corrected for radioimpurities, acetylcholinesterase activity and non- $[^3\text{H}]\text{AcCh}$ radioactivity [9].

Fig. 2. Detergent effect on α -Btx binding. β_2 is the degree of binding of the second α -Btx molecule to nAcChR of *T. californica* membrane fragments. $[D]$ is the concentration of Triton X-100 at 4°C . 30 mM NaCl, 1 mM CaCl_2 , 4 mM KCl, 4 mM Na phosphate, 1 mM Pipes, 0.05 mM EDTA, 0.3 mM NaN_3 , pH 7. Initial (at $[D] = 0$) concentration of AcChR (in terms of $M_r = 290000$): $[R_T] = [BR]_0 = 0.03 \mu\text{M}$; concentration of α -Btx: $[B_T] = 0.24 \mu\text{M}$. Equilibrium constants of α -Btx binding: $K_1 \approx K_2 = 10^{-11} \text{M}$.

affinity conformers is dependent on the way the acetylcholine concentration is increased (simple mixing versus dialysis).

In the present study, the existence of scanning curves [7,8] is shown. The kinetics of AcCh binding under dialysis conditions [10] and the detergent-induced binding of a second α -bungarotoxin molecule [1,11,12] to nAcChR in the membrane fragments are analysed. The main result is that the final very high affinity conformer R_{vh} does not pre-exist in its unliganded form. Rather, it is induced by AcCh binding and is only stable as the acetylcholine binding complex AR_{vh} .

MATERIALS AND METHODS

The method of preparing AcChR-rich membrane fragments from *Torpedo californica* electric organ was that of Sobel et al. [13] with some modifications [1]. The total nAcChR concentration $[R_T]$ was determined from the number of ^{125}I - α -bungarotoxin (α -Btx) sites measured by the DE-81 (Whatman) filter disk method [14] (see also ref. 1). Acetylcholinesterase activity of the membrane fragments was assayed by the Ellman test; Tetram and DFP were used to block the enzyme [1]. In the pulse mode addition of AcCh, the binding of $[^3\text{H}]\text{AcCh}$ was measured by the ultracentrifugation method. Bound and free AcCh were determined directly. The radiochemical purity of $[^3\text{H}]\text{AcCh}$ was determined by TLC. The $[^3\text{H}]\text{AcCh}$ concentration was corrected for residual esterase activity and non- $[^3\text{H}]\text{AcCh}$ contributions [1].

In the dialysis mode the concentration of free $[^3\text{H}]\text{AcCh}$ inside the dialysis bag changes with time; it had to be determined directly from the bag contents.

RESULTS

Detergent effect on α -bungarotoxin binding

The binding of α -Btx is a well-established method for quantitatively determining nAcChR binding sites. Recently, it has been discovered that when membrane fragments are exposed to 0.1% ($\approx 2 \text{ mM}$) Triton X-100 they bind twice as much α -Btx as they do in the absence of the detergent. Figure 2 shows that increasing amounts of Triton X-100 cause a gradual increase in the binding of a second α -Btx molecule per monomer ($M_r = 290\,000$) of the receptor dimers $R \cdot R$. Titration with Lubrol WX leads to a similar binding curve.

Scanning curves

The hysteresis loops in Fig. 1 appear to increase in size with increasing receptor concentration. Since the scatter of the $[^3\text{H}]\text{AcCh}$ data points is, however, rather large, the present accuracy of the method is not sufficient to argue in terms of a concentration dependence. The half-binding distribution constant Q of the receptor concentration range $[R_T] = 0.4 - 1.0 \mu\text{M}$ is $Q = (4 \pm 2) \times 10^{-8} \text{ M}$; the equilibrium constant is $\bar{K} = 5 \times 10^{-9} \text{ M}$ [1].

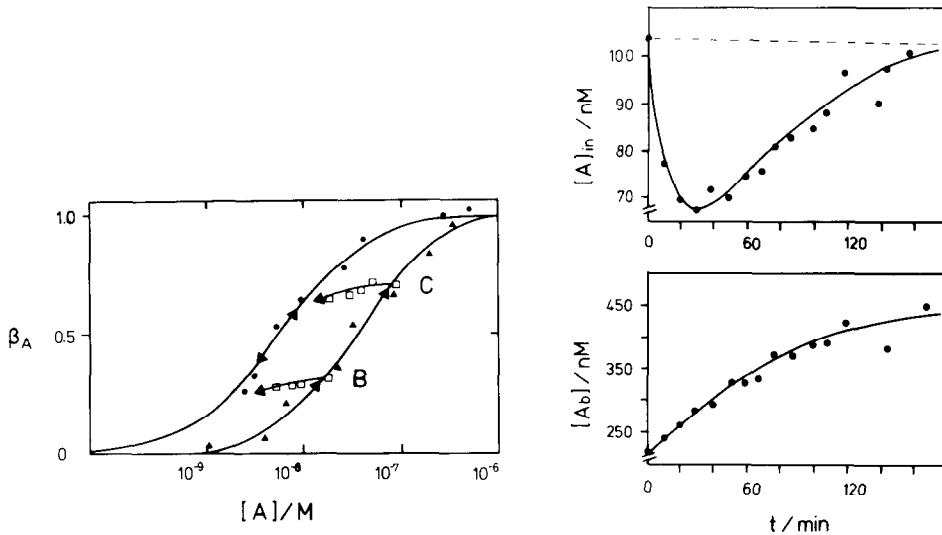


Fig. 3. Two examples of the scanning curves of nAcChR of *T. californica* membrane fragments. Main hysteresis loop of pulse-like addition of AcCh (\blacktriangle , \rightarrow) and of dilution from $[A] > 1 \mu M$ along the equilibrium (dialysis) curve (\bullet , \leftarrow). (\square) Dilution curves starting from the lower hysteresis branch. $[R_T] = 1 \mu M$, $\bar{K} = 5 \times 10^{-9} M$ and $Q \approx 4 \times 10^{-8} M$. See Fig. 1.

Fig. 4. Top: Change in the $[^3H]AcCh$ concentration $[A]_{in}$ of membrane fragments/ $[^3H]AcCh$ solution prepared by the pulse mode, inside the dialysis bag as a function of the dialysis time. At the start of the dialysis at $t = 0$, $[A]_{in} = [A_0]$ and $\beta_A = \beta_0$. Bottom: Time course of additional $[^3H]AcCh$ binding caused by the dialysis. Dashed line: $[A]_{out}$ in the absence of AcChR.

Figure 3 shows two typical scanning curves within the main hysteresis loops. For instance, AcCh was added to membrane fragments to obtain $\beta_A = 0.3$ at $[A] = 4 \times 10^{-8} M$ — point B on the pulse-mode binding curve (lower hysteresis branch). Subsequently the AcCh concentration was decreased by dilution. If the pulse-mode binding curve were an equilibrium curve, the dilution would trace this curve backwards. Instead, the dilution curve enters into the main hysteresis loop as a scanning curve. The same is true for the dilution curve starting at point C.

Kinetics of the dialysis mode $[^3H]AcCh$ binding

Figure 4 shows the time courses of the concentrations of free $[^3H]AcCh$ ($[A]_{in}$) and of the bound $[^3H]AcCh$ ($[A_b]$) both inside the dialysis bag. $[^3H]AcCh$ was added to membrane fragments in the bag (pulse mode), yielding initial values of β_0 and $[A_0]_{in}$ on the lower hysteresis branch. At time zero, the bag was exposed to dialysis conditions.

It can be seen that $[A]_{in}$ first decreases and then increases to the level $[A]_{out}$, the $[^3H]AcCh$ concentration outside the bag. The bound AcCh increases gradually until the equilibrium value on the upper hysteresis branch is reached. It appears that in

the initial phase the additional binding of AcCh is faster than the diffusional supply of AcCh from the outside solution such that $[A]_{in}$ sinks below the level $[A]_{out}$. The characteristic behaviour of $[A]_{in}$ and $[A_b]$ is intrinsic to the open-system condition of the dialysis.

DISCUSSION

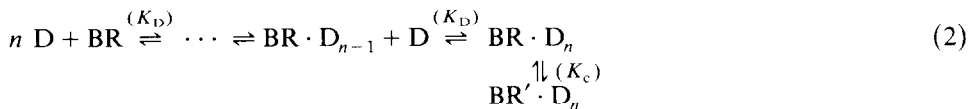
Detergent causes the binding of a second α -Btx molecule

The data in Fig. 2 suggest that detergent binding causes changes in the membrane-bound nAcChR that permit the binding of a second α -Btx molecule. The data can be described in terms of a steric hindrance model for the second α -subunit of the monomer ($M_r \approx 290\,000$). It appears that the increase in the concentration of the detergent removes the hindrance such that the second α -site is also occupied by α -Btx [11].

Whereas in the absence of detergents (D) the binding of α -Btx (B) to the receptor monomer (R) is described globally by



the reaction sequence for the titration of B with D in the presence of an excess of B is given by



The structural transition $R \rightleftharpoons R'$ converts the second α -site into a conformation that binds α -Btx with high affinity as soon as n detergent molecules have bound. Because of the high-affinity binding of the second B molecule the smooth curve in Fig. 2 indicates the independent and allosteric nature of the detergent binding. Reaction (3) apparently does not shift reaction (2), which is only dependent on the concentration of D. The toxin-binding reaction (3) may be used to measure the detergent effect on the receptor. Therefore, the degree of binding of the second α -Btx molecule, $\beta_2 = [B_2R' \cdot D_n]/[R_T]$, relative to the total receptor concentration $[R_T]$ can be related to $[D]$ by [11,12]

$$\beta_2 = \frac{K_c}{1 + K_c} \frac{[D]}{\bar{K}_D + [D]} \quad (4)$$

where $\bar{K}_D = K_D/(1 + K_c)$ is the overall detergent equilibrium dissociation constant. For D = Triton X-100, we obtain at 4°C and the conditions given in the legend of Fig. 2, $\bar{K}_D = 2.8 (\pm 0.3) \times 10^{-4}$ M. In the case of the detergent Lubrol WX, we

obtain $\bar{K}_D = 3.3 (\pm 0.4) \times 10^{-4} M$. These constants are apparent quantities partially reflecting lipid-detergent exchange of the receptor protein.

Domain structure of nAcChR in the membrane fragments

The AcCh binding hysteresis and the existence of scanning curves (see Fig. 3) qualify nAcChR as a physical memory molecule with a co-operative non-equilibrium domain structure [7,8]. The scanning curves are additional evidence for the previous conclusion that the pulse mode addition of AcCh to nAcChR membrane fragments does not yield equilibrium values for β_A and $[A]$. Rather, at the level of high affinity AcCh binding at $[A] \leq 1 \mu M$, simple (non-dialytic) mixing of nAcChR with AcCh leads to non-equilibrium distributions of low and high affinity conformers. The non-equilibrium distribution is extremely long-lived; it may be characterized by a half-binding constant Q . However, any equilibrium analysis of the pulse mode data in terms of equilibrium binding co-operativity (upward curvature of Scatchard plots) is forbidden. Already the fact that only *one* AcCh molecule binds to the high affinity receptor conformer in equilibrium excludes any ligand binding co-operativity.

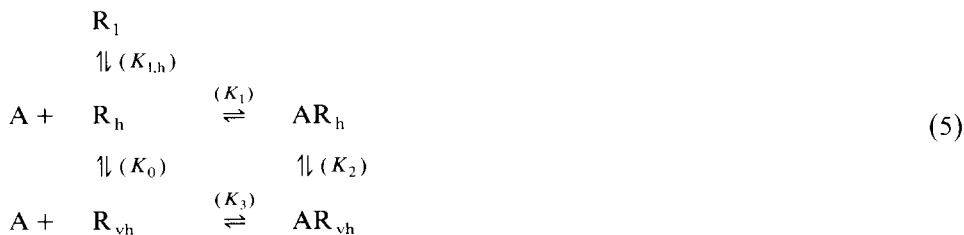
The non-equilibrium co-operativity indicated by hysteresis and scanning [6-8] can be successfully analysed in terms of the receptor dimer concept [1,12,15]. In particular, the notion of a dimer hybrid $R_l \cdot R_h$ has proven to be very useful.

It is known that also in the absence of AcCh binding a conformational equilibrium of the type $R_l \rightleftharpoons R_h$ exists between low affinity (R_l) and high affinity (R_h) conformers. The data suggest that the equilibrium constant K_h of AcCh binding to R_h has a value of about $10^{-7} M$. Therefore, R_h is a conformer of intermediate affinity for AcCh; it is not the final conformer of highest affinity. The data in Fig. 4 suggest that the final receptor conformer, leading to the overall value $\bar{K} = 5 \times 10^{-9} M$ at $4^\circ C$, is only stable in the AcCh binding form AR_{vh} .

[³H]AcCh dialysis kinetics

Cyclic reaction scheme

Kinetic analysis of the dialysis data in Fig. 4 requires a reaction scheme involving R_l ($K_l \approx 10^{-4} M$), R_h ($K_h \approx 10^{-7} M$) and $R_{vh} \ll \bar{K}$). At AcCh concentrations $[A] < 1 \mu M$, AcCh binding to R_l can be neglected ($< 1\%$); hence the minimum reaction scheme for the binding of AcCh in terms of the monomer units R reads:



The induced-fit model

In scheme (5) the final high affinity complex AR_{vh} can be obtained along two limiting pathways. The kinetic analysis will show that only the induced-fit pathway



is consistent with the data. The pathway of direct, selective binding of A to the conformer R_{vh} is negligible, i.e. practically excluded.

The practical, apparent equilibrium constant of the high affinity AcCh binding for the general scheme (5) is given by

$$\bar{K} = \frac{[A]([R_h] + [R_{vh}])}{[AR_h] + [AR_{vh}]} = \frac{K_1(1 + K_0^{-1})}{1 + K_2^{-1}} \quad (7)$$

where the individual apparent equilibrium and rate constants are given by

$$\left. \begin{aligned} K_1 &= [A][R_h]/[AR_h] \\ K_2 &= [AR_h]/[AR_{vh}] = k_{-2}/k_2 \\ K_3 &= [A][R_{vh}]/[AR_{vh}] \\ K_0 &= [R_h]/[R_{vh}] = k_{-0}/k_0 \\ K_{1,h} &= [R_1]/[R_h] \end{aligned} \right\} \quad (8)$$

For the induced-fit model in scheme (6), eqn. (7) is reduced to

$$\bar{K} = K_1/(1 + K_2^{-1}) = K_1 K_2/(1 + K_2) \quad (9)$$

Rate equation

The fundamental rate equation for the slow increase in the concentration of the complex AR_{vh} (observed in Fig. 4) is

$$d[AR_{vh}]/dt = k_2[AR_h] - k_{-2}[AR_{vh}] \quad (10)$$

The degree of total high affinity binding is defined by $\beta = [A_b]/[R_T]$ or explicitly

$$\beta = ([AR_{vh}] + [AR_h])/[R_T] = [AR_{vh}](1 + K_2)/[R_T] \quad (11)$$

Mass conservation implies that the total receptor (binding site) concentration is

$$\begin{aligned} [R_T] &= [R_h] + [R_1] + [AR_h] + [AR_{vh}] \\ &= [R_h](1 + K_{1,h}) + \beta[R_T] \end{aligned} \quad (12)$$

Because of the min/h kinetics indicated in Fig. 4 it is reasonable to assume that the bimolecular binding step (associated with K_1) is fast compared to the slow structural transition (k_2, k_{-2}). Therefore, $[AR_h]$ is given by the pre-equilibrium

$$[AR_h] = K_1^{-1}[A][R_h] \quad (13)$$

Equation (12) yields $[R_h] = (1 - \beta)[R_T]/(1 + K_{1,h})$; substitution into eqn. (13) and then into eqn. (10) finally leads to the practical rate equation

$$d\beta/dt = a \cdot [A](1 - \beta) - k_{-2} \cdot \beta \quad (14)$$

where with eqns. (8) and (9)

$$a = k_2(1 + K_2)/K_1(1 + K_{1,h}) = k_{-2}/\bar{K}(1 + K_{1,h}) \quad (15)$$

Initial rate

It is readily seen that

$$d\beta/dt = -d(1 - \beta)/dt = -(d[A]/dt)/[R_T] \quad (16)$$

At the start of the dialysis at $t = 0$, $\beta = \beta_0$ and $[A]_{in} = [A_0]$, inside the dialysis bag. Because $\bar{K}^{-1} \gg 1$, the initial rate of [3H]AcCh binding at $t = 0$ is given by

$$(d\beta/dt)_0 = a \cdot [A_0](1 - \beta_0) \quad (17)$$

From eqn. (16) we obtain

$$(d[A]/dt)_0 = -a(1 - \beta_0)[R_T] \cdot [A_0] \quad (18)$$

Lumping the experimental quantities together, we may define the relative initial rate:

$$v_0 = -(d[A]/dt)_0/(1 - \beta_0)[R_T] = a[A_0] \quad (19)$$

It can be seen from eqns. (18) and (19) that the induced-fit model in scheme (5) predicts that the initial rate of the decrease in $[A]_{in}$ is proportional to the initial AcCh concentration at the start of the dialysis.

On the other hand, the limiting case of rapid, direct, selective binding $A + R_{vh} \rightleftharpoons AR_{vh}$ coupled to the slow, rate-determining step $R_{vh} \rightleftharpoons R_h$ (k_{-0} , k_0) leads to an expression for the initial relative rate:

$$v_0 = -(d[A]/dt)_0/(1 - \beta_0)[R_T] = k_0 \quad (20)$$

This means that v_0 is a constant, independent of $[A_0]$. Although analysis of the dialysis data according to eqn. (19) is rather inaccurate because of the inaccuracy of graphical slope determinations, Fig. 5 shows clearly that the v_0 values are dependent on $[A_0]$. The linear approximation yields $a \approx 3 \times 10^{-4} \text{ nM}^{-1} \text{ min}^{-1}$.

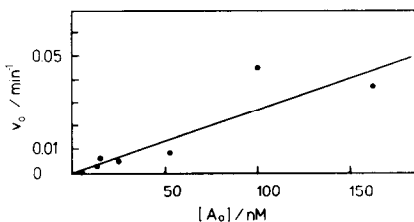


Fig. 5. Initial relative rate v_0 as a function of the initial AcCh concentration $[A_0]$ in the dialysis bag. See eqn. (19) in the text.

Integral rate equation

Because two sets of data, $[A]$ and $\beta = \beta_A$, are available for every time point the entire time courses, $[A(t)]$ and $\beta(t)$, may be treated analytically. For this purpose, eqn. (14) is rewritten as

$$d\beta/dt = a[A] - a([A] + \bar{K})\beta \quad (21)$$

Equation (21) is an inhomogeneous differential equation, solved by first solving the homogeneous form $d\beta/dt = -a([A] + \bar{K})\beta$ yielding $\beta = C \exp[-a \int ([A] + \bar{K}) dt]$, where C is an integration constant.

By the method of variation of C , we obtain within the integration boundaries t and $t_0 = 0$, β and $\beta(t=0) = \beta_0$:

$$\beta = \left(a \int [A] \exp \left[a \int ([A] + \bar{K}) dt \right] dt + \beta_0 \right) \exp \left[-a \int ([A] + \bar{K}) dt \right] \quad (22)$$

The available database permits a graphical evaluation replacing the integrals by sums according to

$$\int_0^t [A(t)] dt = \sum_{i=1} [\bar{A}_i] \Delta t_i \quad (23)$$

where

$$[\bar{A}_i] = ([A]_i - [A]_{i-1})/2$$

and

$$\Delta t_i = t_i - t_{i-1}$$

with $t_{i-1} = t_0$ at $i = 1$.

Introducing the terms

$$y = \beta - \beta_0 \cdot b \quad (24)$$

$$x = \left(\sum [\bar{A}_i] \exp \left[a \sum ([\bar{A}_j] + \bar{K}) \Delta t_j \right]_i \cdot \Delta t_i \right) b \quad (25)$$

$$b = \exp \left[-a \sum ([\bar{A}_i] + \bar{K}) \Delta t_i \right] \quad (26)$$

the dialysis data can be evaluated according to $y = ax$. As shown in Fig. 6, the dependence is linear, yielding $a = 6.5 \times 10^{-4} \text{ nM}^{-1} \text{ min}^{-1}$.

The fraction of R_1 conformers (at $[A] = 0$) was estimated to be ≈ 0.8 [16]; thus, $K_{1,h} \approx 0.8/0.2 = 4$. From eqn. (15), we obtain $k_{-2} = a\bar{K}(1 + K_{1,h}) \approx (2.7 \pm 0.2) \times 10^{-4} \text{ s}^{-1}$. Since $[AR_{v,h}]$ appears to be large compared with $[AR_h]$, it is obvious that $K_2^{-1} \ll 1$; therefore, $\bar{K} \approx K_1 K_2 = K_1 \cdot k_{-2}/k_2$. If we take the estimate $K_1 \approx 10^{-7} M$, we find $k_2 \approx K_1 k_{-2}/\bar{K} \approx 5.4 \times 10^{-3} \text{ s}^{-1}$ and $K_2 \approx 0.05$. The numerical values of $k_2 \approx 5.4 \times 10^{-3} \text{ s}^{-1}$ and $k_{-2} \approx 0.27 \times 10^{-3} \text{ s}^{-1}$ correspond to the rather slow kinetics of the additional AcCh binding under dialysis conditions. The intrinsic relaxation rate of the $AR_h \rightleftharpoons AR_{v,h}$ equilibration is given by $1/\tau = k_2 + k_{-2} \approx 5.67 \times 10^{-3} \text{ s}^{-1}$ or $\tau \approx 3 \text{ min}$. This value may be compared to the time constant of AcCh equilibration across the dialysis bag in the absence of binding (no membrane fragments): $\tau_{eq} \approx 30 \text{ min}$ [10]. Therefore, the kinetics of $[A]$ changes in the presence

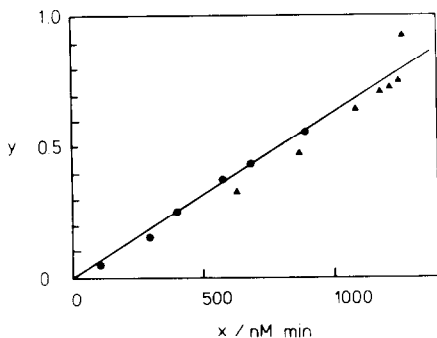


Fig. 6. Dialysis data evaluation according to $y = ax$ derived from eqn. (22). (●, ▲) Two different protein concentrations.

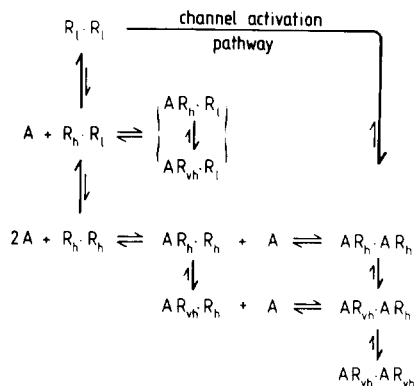


Fig. 7. Reaction scheme of high affinity AcCh binding to *T. californica* nAChR. The simple bimolecular processes are represented by the horizontal sequences, whereas the vertical steps model the various slow structural isomerizations. R_1 : low affinity conformer ($K_1 \approx 10^{-4} M$); R_h : high affinity conformer ($K_h \approx 10^{-7} M$); R_{vh} : very high affinity conformer ($K_{vh} \ll \bar{K} = (5 \pm 1) \times 10^{-9} M$). The $R_h \cdot R_1$ hybrid form is the branching point for the dead-end hybrid $AR_{vh} \cdot R_1$ of the pulse-mode non-equilibrium states. The thick arrows indicate the preferential position of the isomerization equilibria. The large upper arrow indicates the channel activation pathway. At high AcCh concentrations ($> 10^{-6} M$), the low affinity conformer R_1 is directly involved in the binding which results in channel opening and, under prolonged exposure to AcCh, it is subsequently transformed into high affinity conformers. At low AcCh concentrations $c < 10^{-6} M$, the R_h (and R_{vh}) conformer is the dominant direct reaction partner for AcCh and thus constitutes the direct route of the high affinity state pathway to the final complex AR_{vh} . Hysteresis: “Single pulse mode addition” of AcCh (closed system) favours the hybrid $AR_{vh} \cdot R_1$ binding state, whereas “dialysis mode addition” (open system) ultimately leads to the $AR_{vh} \cdot AR_{vh}$ conformer.

of membrane fragments must be rate-limited by the receptor structural changes. The rather dramatic decrease of $[A]_{in}$ within about 30 min after the start of dialysis is caused by the rather limited size of the surface of the dialysis bag limiting the net amount of AcCh which can enter the bag. In the initial dialysis phase, the nAChR-rich membrane fragments bind AcCh more rapidly than the rate of supply by diffusion from the outside of the dialysis bag.

Reaction scheme of the AcCh recognition hysteresis

On the basis of the kinetic data [10], the reaction scheme previously developed to rationalize thermodynamic data [1] can be specified in terms of the induced-fit mechanism, excluding major amounts of direct binding of AcCh to the very high affinity conformer because its concentration is negligibly small (see Fig. 7).

Physiological aspects of the AcCh recognition hysteresis

In cholinergic synapses, nAChR is at a strategically important position of the postsynaptic membrane. According to the present concept, a nerve impulse leads to

the release of AcCh [17]. The AcCh cation binds to the nAcChR membrane receptor and causes a transient structural change [18] to the open channel conformation of this Na^+/K^+ transport-gating protein. The transient cation flux causes membrane depolarization, which may finally trigger action potentials in the subsynaptic cell membrane.

The open channel conformation of the nAcChR protein is short-lived metastable [19]. In the prolonged presence of AcCh, the active channel-open phase spontaneously converts into inactive, desensitized receptor conformers of high and very high affinity for AcCh [20]. It is only the R_1 conformers that are involved in channel activity, most likely as highly co-operative dimers (double-channels), as shown recently [15]. However, due to the conformational coupling ($R_1 \rightleftharpoons R_h$) the low affinity receptor conformers are also affected by the hysteresis of the high affinity conformers.

The longevity of the metastable hybrid conformations $AR_h \cdot R_1$ and $AR_{vh} \cdot R_1$ may be caused by steric hindrance in the dimer preventing the $R_1 \rightarrow R_h$ transition. Functionally, the partially occupied hybrids may be viewed as a saving device for the channel-active R_1 conformers. At low AcCh concentrations ($[A] < 1 \mu M$), hysteresis comprises a mechanism to prevent total conversion to the inactivated, desensitized conformers. It has recently been shown [21] that AcCh binding enhances the phosphorylation of phosphatidylinositol by the isolated nAcChR/lipid complex as well as the autophosphorylation of the receptor. If now the AcCh binding hysteresis is concomitant with a phosphorylation hysteresis, the (desensitized) nAcChR may serve as a memory molecule in the transynaptic information flux through nerve-nerve and nerve-muscle synapses. Thus, the AcCh binding hysteresis may serve as part of the molecular mechanism of synaptic memory imprint and recognition memory.

ACKNOWLEDGEMENTS

We thank M. Pohlmann for typing the manuscript and the Deutsche Forschungsgemeinschaft for financial support (grant D3, SFB 223) to E.N.; grant NS-11766 to H.W.C. is gratefully acknowledged.

REFERENCES

- 1 H.W. Chang, E. Bock and E. Neumann, *Biochemistry*, 23 (1984) 4546.
- 2 M. Spodheim and E. Neumann, *Biophys. Chem.*, 3 (1975) 109.
- 3 D. Thiele and W. Guschlbauer, *Biopolymers*, 8 (1969) 361.
- 4 A. Katchalsky and R. Spangler, *Q. Rev. Biophys.*, 1 (1968) 127.
- 5 A. Katchalsky and E. Neumann, *Int. J. Neurosci.*, 3 (1972) 175.
- 6 E. Neumann, *Angew. Chem.*, 85 (1973) 430; *Angew. Chem., Int. Ed. Engl.*, 12 (1973) 356.
- 7 D.H. Everett, *Trans. Faraday Soc.*, 51 (1955) 1551.
- 8 D.H. Everett in E.A. Flood (Ed.), *The Solid-Gas Interface*, Vol. 2, Marcel Dekker, New York, 1967, p. 1055.
- 9 H. Wolf, Diploma thesis, University of Bielefeld, 1986.

- 10 B. Rauer, Diploma thesis, University of Bielefeld, 1987.
- 11 E. Boldt, Diploma thesis, University of Bielefeld, 1986.
- 12 E. Neumann, in Maelicke (Ed.), *Nicotinic Acetylcholine Receptor*, NATO ASI Series, Vol. H3, 1986, pp. 177–196.
- 13 A. Sobel, M. Weber and J.P. Changeux, *Eur. J. Biochem.*, 55 (1975) 505.
- 14 H.W. Chang and E. Bock, *Biochemistry*, 16 (1977) 4513.
- 15 N.D. Boyd and J.B. Cohen, *Biochemistry*, 19 (1980) 5344.
- 16 B. Katz, *The Release of Neural Transmitter Substances*, Liverpool University Press, Liverpool, 1969, p. 55.
- 17 D. Nachmansohn, *Harvey Lect.*, 49 (1955) 57.
- 18 E. Neumann and J. Bernhardt, *J. Physiol. (Paris)*, 77 (1981) 1061.
- 19 B. Sakmann, J. Patlack and E. Neher, *Nature*, 286 (1980) 71.
- 20 H. Schindler, F. Spillecke and E. Neumann, *Proc. Natl. Acad. Sci. USA*, 81 (1984) 6222.
- 21 R. Kiehl, M. Varsanyi and E. Neumann, *Biochem. Biophys. Res. Commun.*, in press.